Eur. Phys. J. B **15**, 3–6 (2000)

THE EUROPEAN PHYSICAL JOURNAL B

EDP Sciences

Rapid Note

Parametric stabilization of the Rosensweig instability

F. Pétrélis, É. Falcon[a], and S. Fauve[b]

Laboratoire de Physique Statistique[c], École Normale Supérieure, 24 rue Lhomond, 75231 Paris Cedex 05, France

Received 29 November 1999

Abstract. We report an experimental study of the inhibition of the instability generated by a magnetic field applied perpendicularly to the surface of a magnetic fluid (the Rosensweig instability), by vertical vibrations of the fluid container. Our measurements are in quantitative agreement with a simple analytical model using the theory of Mathieu functions.

PACS. 47.20.-k Hydrodynamic stability – 75.50.Mm Magnetic liquids – 47.35.+i Hydrodynamics waves – 47.54.+r Pattern selection; pattern formation

Parametric stabilization is a well known phenomenon in the theory of the Mathieu oscillator [1]. A canonical example is the inverted pendulum, whose unstable upright position could be stabilized by vertically vibrating its point of suspension; this physical mechanism has been used in various devices, for instance the Paul trap that allows the confinement of an electric charge in a quadrupolar time periodic electric field [2]. Parametric stabilization has been also observed in fluid dynamics, the most impressive example being the inhibition of the Rayleigh-Taylor instability: a horizontal fluid layer could be stabilized above an other one of smaller density, by vertically vibrating their container [3]. However, this requires a container with a rather small horizontal extension because modes with a large enough wavelength are not parametrically stabilized. It has been predicted recently that the Rosensweig instability, *i.e.* the stationary instability of a layer of ferrofluid submitted to a normal magnetic field [4], could be inhibited by vertical vibrations with an appropriate choice of the fluid and vibration parameters [5]. We report the experimental observation of this effect and determine the parametric and Rosensweig instability thresholds in parameter space (acceleration amplitude and frequency and magnetic induction). We understand most of our observations with a simple analytical model using the theory of Mathieu functions.

The experimental setup consists of a vertically vibrating cylindrical vessel, 8.5 cm in inner diameter and 1 cm in depth. An electromagnetic vibration exciter (BK4810) drives the container sinusoidally in the frequency range from 30 to 70 Hz. The vertical acceleration amplitude, A, is measured by means of a piezoelectric accelerometer (BK4393V). The container is filled with 25 ml to 37 ml of magnetic fluid APG512A, Lot. N° F5136C (Ferrofluidics), corresponding to a depth h of ferrofluid from $h = 4.4$ mm to $h = 6.5$ mm. The properties of the fluid are: density, $\rho = 1.26$ g/cm^3, surface tension, $\gamma = 35 \times 10^{-3}$ N/m, initial magnetic susceptibility, $\chi_{\rm i} = 1.4$, saturation moment, $M_{\rm sat} = 300$ gauss, and dynamic viscosity, $\eta = 75$ mPa s [6]. The whole setup is placed between a pair of Helmholtz coils, 16 cm (resp. 36 cm) in inner (resp. outer) diameter, 8.4 cm far apart. A DC current up to 6 A is supplied to the coils by a generator (KEPCO BOP36-6M). The magnetic induction is measured by means of a Hall probe (HP1755), located in the center near the surface of the vessel, and is found to be a linear function of the applied current with a 50 gauss/A slope. This slope is independent of the presence of the ferrofluid and the electromagnetic exciter. Our control parameters are the applied magnetic induction B, the driving frequency f, and the dimensionless acceleration amplitude $\Gamma = A/g_0$ ranging from 0 to 10, where $g_0 = 9.81$ m/s^2 is the acceleration due to gravity. The motions of the free–surface of the ferrofluid are visualized with a video camera mounted above the center of the vessel. A typical pattern at large enough vibration amplitude and magnetic field is displayed in Figure 1. The hexagonal pattern is generated by the Rosensweig instability. The modulation visible on the lines between two adjacent hexagons correspond to subharmonic waves generated by the Faraday instability.

Experiments are conducted at a fixed value of the driving frequency, by increasing or decreasing Γ (resp. B)

[a] *Present address*: Laboratoire de Physique, École Normale Supérieure de Lyon, 46 allée d'Italie, 69364 Lyon Cedex 07, France

[b] e-mail: `fauve@physique.ens.fr`

[c] CNRS, UMR 8550

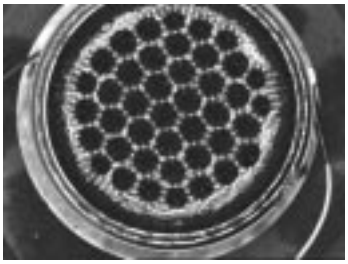

Fig. 1. Photograph of the fluid surface seen from above.

at a fixed value of B (resp. Γ). Figure 2 shows the thresholds for the subharmonic Faraday instability and the Rosensweig instability *versus* the dimensionless acceleration Γ and the magnetic induction B at an excitation frequency $f = 40$ Hz. Two measurements of Γ (respectively B) are performed, one just below onset when the interface is flat, and the other just above onset, when patterns are present. Their difference gives the error bars on the critical acceleration and magnetic induction measurements, ± 1 m/s^2, respectively ± 2 gauss.

Without parametric excitation, the magnetic induction threshold for the Rosensweig instability is $B_c = 151 \pm 2$ gauss in agreement with the theoretical value (see below). The instability nucleates in the center of the cell because the magnetic field is slightly larger there, and generates an hexagonal pattern. It is known to be a subcritical instability but our measurements are not precise enough to study the corresponding hysteresis cycle. It is clear from Figure 2 that parametric excitation can delay the Rosensweig instability onset to larger values of the critical magnetic induction $B_c(\Gamma)$, *i.e.* stabilizes the flat surface. The instability wavenumber k_c stays roughly constant along the marginal curve $B_c(\Gamma)$. The increase that one may expect because of the increase of $B_c(\Gamma)$ with Γ is too small with respect to the quantization imposed by the lateral boundaries.

In the absence of magnetic field, the flat surface undergoes the Faraday instability when the vertical vibration, *i.e.* Γ, is large enough. At a given excitation frequency, the critical acceleration Γ_F for instability onset increases when the viscosity and/or the wavenumber increase, because both terms lead to an increase of the dissipation in the deep layer limit [9]. The generated pattern takes the form of a standing plane wave because of the large enough value of the dissipation [10]. It is clear from Figure 2 that the onset of the Faraday instability is delayed when a vertical magnetic field is applied. The instability wavenumber is also an increasing function of the magnetic induction (it increases roughly by a factor 2 along the marginal curve $\Gamma_F(B)$). This results from the modification of the wave dispersion relation by the magnetic field (see Eq. (1) in the discussion below). Since bulk dissipation in the fluid increases proportionally to the square of the wavenumber, the critical acceleration $\Gamma_F(B)$ increases with B.

Figure 2 shows that the marginal stability curves do not depend on the fluid volume *i.e.* on the depth of the fluid layer because we are in the large depth limit ($kh \gg 1$). Thus, the modification of the shape of the meniscus

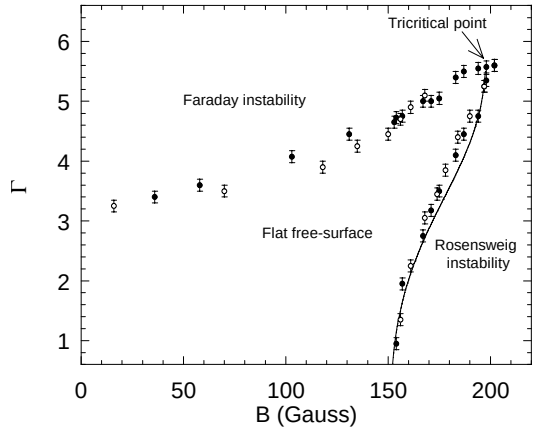

Fig. 2. Stability thresholds for the Faraday instability and the Rosensweig instability as a function of the dimensionless acceleration Γ and the magnetic induction B. Excitation frequency $f = 40$ Hz; volume of ferrofluid: 25 ml (•), 35 ml (○). The solid line corresponds to equation (8) without any adjustable parameter.

of the ferrofluid under the action of the magnetic field and the corresponding slight variation of the height of the layer, cannot contribute to the increase of $\Gamma_F(B)$ with B. It is not necessary either to invoke the dependence of the rotational viscosity of the ferrofluid on the magnetic field [8].

The point where the marginal curves of the Rosensweig and Faraday instabilities intersect, (Γ_t, B_t), can be called a *tricritical point* using the language of phase transitions. The Rosensweig instability cannot be stabilized by parametric forcing for $B > B_t$. The phase diagram displayed in Figure 2 remains qualitatively unchanged (up to a shift of the marginal curves) when the vibration frequency is varied in the range $30 < f < 70$ Hz. No stabilization of the Rosensweig instability is observed when the frequency is too low. The high frequency limit is due to the limited power of our vibration exciter. The linear stability of a vertically vibrated layer of viscous ferrofluid submitted to a vertical magnetic field has been recently studied by Müller [5]. His calculations showed that the Rosensweig instability can be parametrically stabilized at high enough shaking frequency, in agreement with our experimental observations. The threshold of the Faraday instability looks almost not affected by the magnetic field amplitude (Fig. 7a of his paper) whereas we observe that it increases because of the change in wavenumber due to the magnetic field. This is due to the resolution of his plot; a slight increase does exist [11].

We next consider the dependence of the marginal stability curves of Figure 2 on the excitation frequency f. Figure 3 shows that the critical dimensionless acceleration, $\Gamma_c(B)$, for the inhibition of the Rosensweig instability generated by a fixed magnetic induction B, is a linear function of f. The frequency dependence of the coordinates of the tricritical point, (Γ_t, B_t), is displayed in Figure 4. Both Γ_t and B_t are increasing functions of f in our frequency range.

Most of these experimental results can be understood in a simple way using the inviscid theory of the Faraday

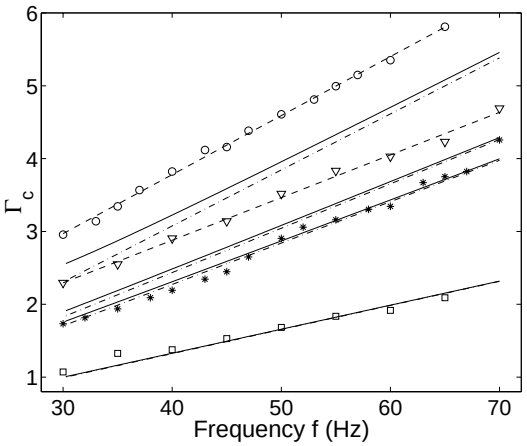

Fig. 3. Critical dimensionless acceleration, Γ_c, for inhibiting the Rosensweig instability, as a function of the driving frequency, f, for various values of the applied magnetic induction $B = 155$ (□), 163 (⋆), 165 (▽) and 175 (○) gauss. Solid (resp. dot–dashed) lines from bottom to top correspond to equation (8) (resp. Eq. (11)) for the same values of B. Dashed lines are linear fits of the experimental data for $B = 165$ and 175 gauss. The volume of ferrofluid is 25 ml. The agreement between experiments and theory is good up to $B = 163$ gauss.

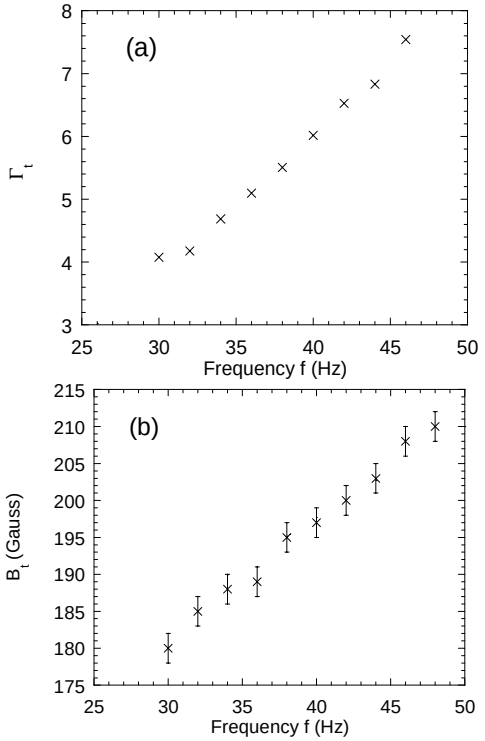

Fig. 4. (a) Dimensionless acceleration, Γ_t, and (b) magnetic induction, B_t, at the tricritical point (see Fig. 2) *versus* the driving frequency. The volume of ferrofluid is 25 ml.

instability [12], taking into account the modification of the surface wave dispersion relation due to the applied magnetic field. We consider the interface between an horizontally unbounded ferrofluid layer of height h and air at atmospheric pressure. The fluid is assumed incompressible, of density ρ and is submitted to a static magnetic induction B perpendicular to its surface. We consider the deep layer approximation which is fulfilled for wavenumbers k such that $kh \gg 1$. Neglecting the fluid viscosity leads to the dispersion relation [4,6],

$$\omega_0^2(k) = \left[g_0 k - \frac{\chi^2}{\rho\mu_0(2+\chi)(1+\chi)} B^2 k^2 + \frac{\gamma}{\rho} k^3 \right] , \quad (1)$$

where ω_0 is the eigenfrequency in the absence of driving, $\mu_0 = 4\pi \times 10^{-7}$ H/m is the magnetic permeability of vacuum, and χ is the magnetic susceptibility of the ferrofluid which depends on the applied magnetic field, H, through Langevin's classical theory [6]

$$\chi(H) = \frac{M_{\rm sat}}{\mu_0 H} \left[\coth\left(\frac{3\mu_0 H \chi_{\rm i}}{M_{\rm sat}} \right) - \frac{M_{\rm sat}}{3\mu_0 H \chi_{\rm i}} \right] , \quad (2)$$

and therefore on the magnetic induction, B, through an implicit equation since

$$B = \mu_0(1+\chi)H. \quad (3)$$

In a static normal magnetic induction, the surface of the magnetic fluid undergoes a stationary instability, the so–called Rosensweig instability, when $\omega_0^2(k)$ becomes negative [4,6]. This condition gives the magnetic induction threshold, B_c,

$$B_c^2 = 2\mu_0 \sqrt{\rho g \gamma} \frac{(2+\chi)(1+\chi)}{\chi^2} , \quad (4)$$

where $\chi(H_c)$ is determined by solving equations (2) together with (3) and (4). Equation (4) yields the critical induction, $B_c = 152$ gauss, in agreement with our experimental value in the absence of driving.

When the fluid is vertically vibrated, the effective gravity becomes $g(t) = g_0 + A\cos(2\pi f t)$, where A and f are the driving acceleration amplitude and frequency. Linear stability analysis [12] shows that an eigenmode of wavenumber k of the surface deformation ζ, obeys the following Mathieu equation,

$$\frac{\partial^2 \zeta}{\partial t^2} + \omega_0^2 \zeta = Ak\zeta \cos(2\pi f t) . \quad (5)$$

Setting $\tau = \pi f t$, $\alpha = -Ak/(\pi f)^2$ and $\beta = \omega_0^2/(\pi f)^2$, we transform (5) into the standard form of the Mathieu equation,

$$\frac{\partial^2 \zeta}{\partial \tau^2} + (\beta + \alpha \cos 2\tau)\, \zeta = 0 . \quad (6)$$

Analysis of (6) in the α–β plane yields a set of unstable and stable regions limited by $\alpha(\beta)$ curves corresponding to periodic solutions of (6), called *Mathieu functions*, which can be expressed in term of series of trigonometric functions [1]. In the vicinity of the ($\alpha = 0$, $\beta = 0$) point, the marginal curves of stability, $\alpha(\beta)$, reduce to [1]

$$\beta \simeq -\frac{\alpha^2}{8} + \frac{7\alpha^4}{2048} , \quad (7)$$

which corresponds in the (Γ, B) plane to the marginal stability curve of the Rosensweig instability near ($\Gamma = 0$, $B = B_c$) (see Fig. 2). Since β is a function of the wavenumber k, we assume that the minimum, $k_{\rm min}$, of the function $\beta(k)$, *i.e.* of $\omega_0^2(k)$, governs the behavior of

the interface when the excitation, *i.e.* α, increases. In other words, we assume that the Rosensweig instability is inhibited by parametric forcing when its most unstable wavenumber in the absence of forcing is inhibited by the external vibration. Using this assumption and inserting the expressions of α and β in (7) leads to a critical value of the driving acceleration amplitude, A_c, for which the Rosensweig instability is inhibited

$$\Gamma_c \equiv \frac{A_c}{g} = \sqrt{\frac{8}{7}}\frac{(2\pi f)^2}{g k_{\min}}\sqrt{1-\sqrt{1+\frac{7}{8}\frac{\omega_0^2(k_{\min})}{(\pi f)^2}}}, \qquad (8)$$

with $-8\pi^2 f^2/7 \leq \omega_0^2(k_{\min}) \leq 0$,

$$k_{\min} = \frac{1}{3}\sqrt{\frac{\rho g}{\gamma}}\left(u+\sqrt{u^2-3}\right), \qquad (9)$$

and

$$u \equiv \frac{\chi^2}{(1+\chi)(2+\chi)}\frac{B^2}{\mu_0\sqrt{\rho g \gamma}}\,. \qquad (10)$$

The critical dimensionless acceleration, Γ_c, predicted by (8) is plotted in Figure 2 (solid line) without any adjustable parameter. The agreement is perfect up to $B = 163$ gauss. More surprisingly, since our approximation is valid only in the vicinity of ($\Gamma = 0$, $B = B_c$), the whole marginal stability curve of the Rosensweig instability in the presence of parametric forcing is rather well described by (8) up to the tricritical point. The limited accuracy of (8) when B increases is more visible in Figure 3. Although the linear dependence of Γ_c *versus* f is displayed by our model, its quantitative agreement with the experiments is observed only up to $B = 163$ gauss. Note that the second order approximation in our model (Eq. (8), solid lines) is not much better that the first order one (dot-dashed lines), which consists of neglecting the term in α^4 in (7) and gives

$$\Gamma_c \simeq \sqrt{2}\frac{(2\pi f)}{g k_{\min}}|\omega_0(k_{\min})|. \qquad (11)$$

We can use this latest expression to get an experimental determination of the magnetic susceptibility of the ferrofluid, χ, as a function of B (Fig. 5). Substituting (9) into (11) together with (1) leads to $\Gamma_c \simeq Cf$ where

$$C^2 \equiv \frac{8\pi^2}{3}\sqrt{\frac{\gamma}{\rho g^3}}\left(2\sqrt{u^2-3}-u\right)\,, \qquad (12)$$

where u is given by (10). Identifying the expression of C to the slope of each Γ_c *vs.* f lines (only some of them have been displayed in Figure 3 for clarity), and solving this equation, leads to the experimental determination of the magnetic susceptibility of the ferrofluid, $\chi(B)$. These experimental values ($\times$) are compared to the theoretical value (solid line) given by Langevin's classical theory (2). The agreement is satisfactory at low enough B, *i.e.* $B \leq 163$ gauss, for which, as already mentioned, (11) is a good approximation.

Various aspects of parametric instabilities have been recently studied using magnetic fluids [13]. We have shown that a vibrated ferrofluid submitted to a static normal magnetic field provides one of the simplest experimental configuration to study quantitatively the mechanism of parametric inhibition of an extended spatial pattern generated by an hydrodynamic instability. Possible extensions of this work are

- the study of the nonlinear couplings between the Rosensweig and Faraday instabilities and their influence on pattern formation in the vicinity of the tricritical point, in particular the study of the destruction of the hexagonal order by the Faraday waves when the vibration amplitude is increased with $B > B_t$,
- the measurement of the threshold of Faraday waves in thin layers of ferrofluids submitted to a normal magnetic field, in order to try to determine the rotational viscosity of a ferrofluid and its dependence on the magnetic field and the frequency.

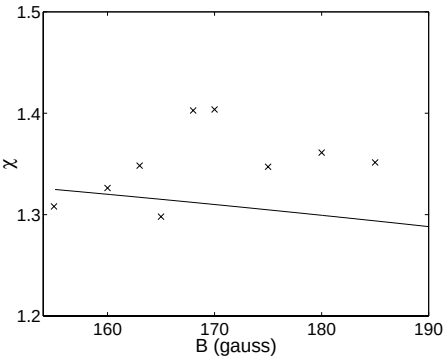

Fig. 5. Magnetic susceptibility χ as a function of the magnetic induction B: experimental determination ($\times$), Langevin's theory equation (2) (solid line).

References

1. see for instance, J. Mathews, R.L. Walker, *Mathematical Methods of Physics* (W.A. Benjamin, Inc., New York, 1964) pp. 189–195.
2. L. Ruby, Am. J. Phys. **64**, 39 (1996) and references therein.
3. G.H. Wolf, Phys. Rev. Lett. **24**, 444 (1970).
4. M.D. Cowley, R.E. Rosensweig, J. Fluid Mech. **30**, 671 (1967).
5. H.W. Müller, Phys. Rev. E **58**, 6199 (1998).
6. B. Abou, G. Néron de Surgy, J.E. Wesfreid, J. Phys. II France **7**, 1159 (1997).
7. A.G. Gailitis, J. Fluid Mech. **82**, 401 (1977).
8. R.E. Rosensweig, *Ferrohydrodynamics* (Dover, New York, 1997) and references therein.
9. S. Fauve, in *Free Surface Flows*, edited by H.C. Kuhlmann, H-J. Rath (Springer, Wien, New York, 1999), pp. 30-32.
10. S. Fauve, K. Kumar, C. Laroche, Y. Garrabos, D. Beysens, Phys. Rev. Lett. **68**, 3160 (1992); W.S. Edwards, S. Fauve, J. Fluid Mech. **278**, 123-148 (1994).
11. H.W. Müller (private communication).
12. T.B. Benjamin, F. Ursell, Proc. Roy. Soc Lond. A **225**, 505 (1954); P.L. Hansen, P. Alstrom, J. Fluid Mech. **351**, 301 (1997).
13. M.P. Perry, T.B. Jones, J. Appl. Phys. **46**, 756 (1974); J.-C. Bacri, A. Cebers, J.-C. Dabadie, S. Neveu, R. Perzynski, Europhys. Lett. **27**, 437 (1994); T. Mahr, I. Rehberg, Europhys. Lett. **43**, 22 (1998); T. Mahr, I. Rehberg, Phys. Rev. Lett. **81**, 89 (1998); J. Broaweys, J.-C. Bacri, C. Flament, S. Neveu, R. Perzynski, Eur. Phys. J. B **9**, 335 (1999).